



HAL
open science

Frequency doubling and sum-frequency mixing operation at 469.2, 471, and 473 nm in Nd:YAG

Xu Bin, Patrice Camy, Jean-Louis Doualan, Braud Alain, Cai Zhiping, François Balembois, Richard Moncorgé

► To cite this version:

Xu Bin, Patrice Camy, Jean-Louis Doualan, Braud Alain, Cai Zhiping, et al.. Frequency doubling and sum-frequency mixing operation at 469.2, 471, and 473 nm in Nd:YAG. *Journal of the Optical Society of America B*, 2012, 29 (3), pp.346-350. hal-00671582

HAL Id: hal-00671582

<https://hal-iogs.archives-ouvertes.fr/hal-00671582>

Submitted on 27 Mar 2012

HAL is a multi-disciplinary open access archive for the deposit and dissemination of scientific research documents, whether they are published or not. The documents may come from teaching and research institutions in France or abroad, or from public or private research centers.

L'archive ouverte pluridisciplinaire **HAL**, est destinée au dépôt et à la diffusion de documents scientifiques de niveau recherche, publiés ou non, émanant des établissements d'enseignement et de recherche français ou étrangers, des laboratoires publics ou privés.

Frequency doubling and sum-frequency mixing operation at 469.2, 471, and 473 nm in Nd:YAG

Bin Xu,^{1,2} Patrice Camy,^{1,*} Jean-Louis Doualan,¹ Alain Braud,¹ Zhiping Cai,²
François Balembois,³ and Richard Moncorgé¹

¹Centre de Recherche sur les Ions, les Matériaux et la Photonique (CIMAP), UMR 6252 Commissariat à l'Energie Atomique–CNRS Ecole Nationale Supérieure d'Ingénieurs de Caen, Université de Caen, 14050 Caen, France

²Department of Electronic Engineering, Xiamen University, Xiamen 361005, China

³Laboratoire Charles Fabry de l'Institut d'Optique (LCFIO), UMR CNRS-Institut d'Optique Graduate School, Université de Paris-Sud, 91127 Palaiseau, France

*Corresponding author: patrice.camy@ensicaen.fr

Received October 21, 2011; accepted October 31, 2011;
posted November 10, 2011 (Doc. ID 156833); published February 14, 2012

We report CW blue laser operation at 469.2, 471, and 473 nm by efficient intracavity second-harmonic generation and sum-frequency generation of the $R_2 \rightarrow Z_5$ (938.5 nm) and $R_1 \rightarrow Z_5$ (946 nm) $^4F_{3/2} \rightarrow ^4I_{9/2}$ intermultiplet transitions in Nd:YAG with an LiB_3O_5 nonlinear crystal. Single-wavelength laser operation at 469.2 nm and multi-wavelength operation at 469.2, 471, and 473 nm are obtained with maximum output powers of 1.4 and 0.15 W, respectively, by using a glass etalon as frequency selector. The 469 nm blue laser is an efficient pumping source of Pr^{3+} -doped materials. © 2012 Optical Society of America

OCIS codes: 140.3580, 140.3530, 140.3515.

1. INTRODUCTION

Quasi-three-level laser emissions around 940 nm in neodymium-doped mixed garnets like YGG/YAG/GGG and YSAG/YSAG/GSAG/GSGG have received a great deal of attention in the past decades for different applications [1–4] such as laser remote sensing (differential absorption LIDAR) of atmospheric water vapor (H_2O). Moreover, along with other Nd-doped crystals such as vanadates, and by using intracavity frequency doubling [5–7], they also allow for very efficient laser emissions of blue light around 470 nm, with interesting applications in the fields of high-density optical data storage, color display, submarine communication, and biology.

On the other hand, with the increasing interest for Pr^{3+} -doped materials as laser media for RGB video-projectors, blue lasers with specific wavelengths at around 445, 469, or 479 nm are required to pump these Pr^{3+} -doped laser hosts [8–13]. Gallium nitride (GaN) diode lasers operating around 445 nm offer the most compact and simple pump source for the development of such lasers but are still limited to about 1 W (without any significant improvement over the last three years), and the beam quality of such laser diodes is considerably degraded for powers higher than 500 mW [10,13]. Frequency-doubled optically pumped semiconductor lasers offer the possibility of higher pump powers with a better beam quality, but they remain on demand, noncommercially available thus rather expensive laser devices.

For these reasons, we show here the details of an alternative solution, which is a simple, efficient, and potentially powerful solid-state laser based on a diode-pumped and intracavity frequency-doubled three-level Nd:YAG laser emitting at 469.2 nm, thus right at the wavelength corresponding to an absorption band of Pr^{3+} [14]. For that purpose the laser has to work on the 938.5 nm transition line of Nd:YAG, which has been far less studied than the 946 nm one. In fact,

such laser emission was first reported by Koch *et al.* [15], and second-harmonic generation (SHG) at 469.2 nm was first demonstrated by Bjurshagen *et al.* [16], but only with a maximum output power of 200 mW by using a periodically poled potassium titanyl phosphate frequency doubler and a Z-type laser resonator. In the present communication, we report on a substantial improvement in the laser output power at this blue laser wavelength by using a compact V-type cavity. We also report, for the first time to our knowledge, 946 and 938.5 nm dual IR laser emission, 471 nm blue laser emission resulting from frequency summing, and simultaneous blue laser emission at about 469, 471, and 473 nm by using an intracavity glass etalon as frequency selector.

2. EXPERIMENTAL CONDITIONS

The experimental setup is shown schematically in Fig. 1. The laser crystal is a 3 mm × 3 mm × 3 mm, 0.5% Nd-doped YAG. No particular effort has been made to optimize the Nd^{3+} doping concentration and crystal length. However, we have considered that a relatively low concentration should be advantageous for alleviating thermal loading [6,17] compared to more commonly used ~1% Nd-doped crystals. The crystal was wrapped into an indium foil and mounted on a copper heat sink. The temperature of the laser crystal cooled by flowing water was maintained at 8 °C with an accuracy of ±0.2 °C. A 30 W fiber-coupled laser diode emitting around 808 nm was used as the pump source. The end of the fiber has a 200 μm core diameter and an N.A. of 0.22. To optimize the absorption in the crystal, the temperature of the diode was adjusted to 29.7 °C (±0.2 °C). So, at the maximum output power, the pump wavelength was 807.8 nm, with a spectral width (FWHM) of around 2.2 nm. Under these conditions, the crystal absorbed around 37% of the pump radiation. With a collimating doublet of 35 mm focal length and a focusing doublet of

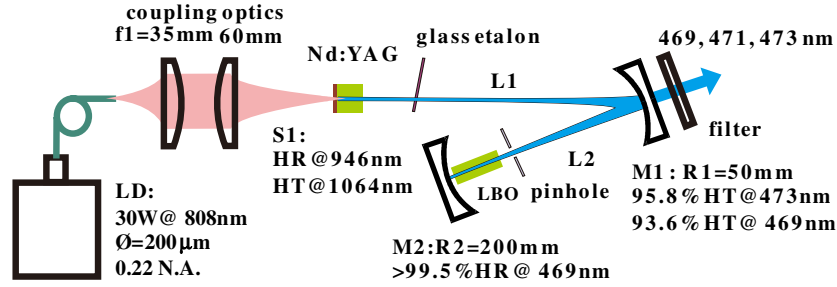


Fig. 1. (Color online) Laser experimental setup. LD, laser diode; f1, focal lengths; S1, coating on the YAG surface; HR, high reflection; HT, high transmission; M1, mirror 1; M2, mirror 2.

60 mm focal length, the end face of the fiber was imaged into the laser crystal with a spot radius of $170 \mu\text{m}$. The left-hand side of the laser crystal acted as the input resonator mirror thanks to a high reflection coating at 938–946 nm and a high transmission coating at 1064 nm. The right-hand side was anti-reflection coated at 900–1100 nm. A 15 mm long LiB_3O_5 (LBO) crystal cut for type I critical phase-matching condition ($\theta = 90^\circ$, $\varphi = 19.9^\circ$ at 303 K for 469 nm) and mounted in a water-cooled copper holder was used for frequency doubling. A pinhole was also inserted before the LBO crystal to avoid the thermal heating of the copper holder arising from the residual pump radiation. This V-shaped cavity was designed to be stable by using the standard ABCD matrix method. After a slight readjustment of the designed arm lengths upon laser operation, the cavity arm lengths L1 and L2 were found to be optimal at 68 and 35 mm, respectively.

As the 938.5 nm laser line has a stimulated emission cross section about 10% weaker than the 946 nm one [18], an appropriate selective element, namely a simple glass plate serving as etalon, was inserted inside the laser cavity to enforce laser operation on one line or the other or both. The glass etalon had a thickness $d = 0.15 \text{ mm}$ and a refractive index $n = 1.45$

3. LBO PHASE MATCHING

For low conversion efficiencies, the second harmonic versus the fundamental wave optical power can be approximated by the expression [19]

$$P_{2\omega} = 2l^2\eta^3\omega^2d_{\text{eff}}^2 \frac{P_\omega^2}{A} \sin^2\left(\frac{\Delta k l}{2}\right), \quad (1)$$

where l is the length of nonlinear crystal, η the plane-wave impedance, d_{eff} the effective nonlinear coefficient, and ω and A the angular frequency and the area of the fundamental beam, respectively. From Eq. (1), one can see that, for a certain nonlinear crystal, the power of the second-harmonic wave mainly depends on the intracavity fundamental power P_ω and the phase mismatch Δk . The \sin^2 term in Eq. (1) is also called normalized SHG conversion efficiency. The phase mismatch Δk can be also expanded in a Taylor series as

$$\begin{aligned} \Delta k &= \Delta k(\Delta\phi, \Delta\lambda, \Delta T) \\ &\approx \Delta k(0) + \left. \frac{\partial(\Delta k)}{\partial T} \right|_{pm} \Delta T + \left. \frac{\partial(\Delta k)}{\partial \phi} \right|_{pm} \Delta\phi + \left. \frac{\partial(\Delta k)}{\partial \lambda} \right|_{pm} \Delta\lambda, \end{aligned} \quad (2)$$

where $\Delta k(0) = 0$ corresponds to perfect phase matching, which means that $\Delta\phi = \Delta\lambda = \Delta T = 0$ and that the maximum output power should be achieved at the operating wavelength. From Eq. (2), the phase mismatch due to one parameter, e.g., $\Delta\lambda$, can be compensated by enforcing phase mismatch onto other parameters, e.g., $\Delta\phi$ or ΔT or both. Figure 2 shows the normalized SHG conversion efficiency of LBO, which was designed for a 938.5 nm fundamental wave. When angular and temperature phase matching are satisfied, i.e., $\Delta T = \Delta\phi = 0$, the FWHM of the sinc function is about 0.58 nm in the blue region (1.16 nm for the fundamental wave). It is apparent that, when keeping constant the angle and temperature of the

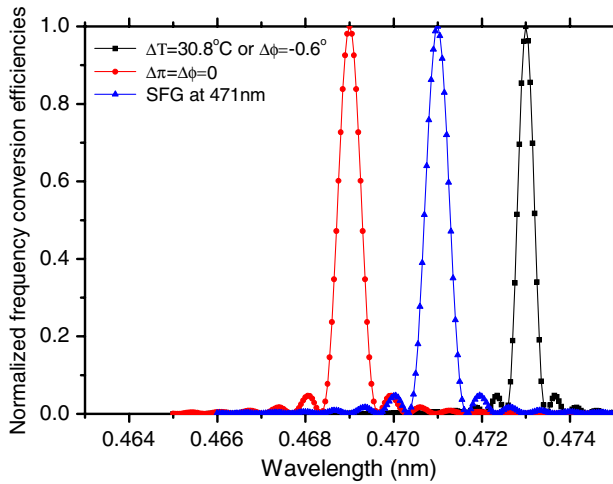


Fig. 2. (Color online) Simulations of normalized frequency conversion efficiencies at 469, 471, and 473 nm for the LBO crystal used in the experiments.

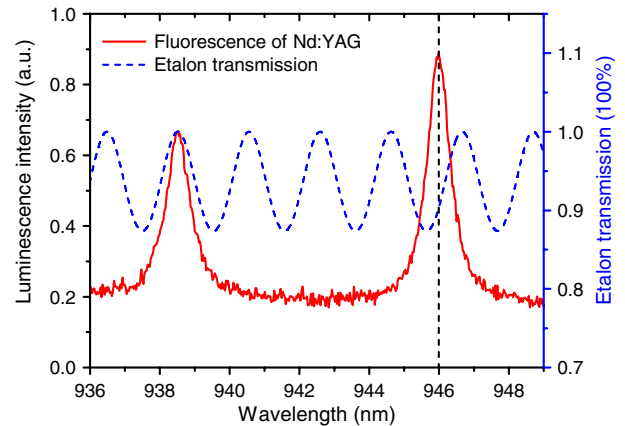


Fig. 3. (Color online) Nd:YAG luminescence spectrum versus calculated etalon transmission with a tilted angle of $\sim 8.8^\circ$.

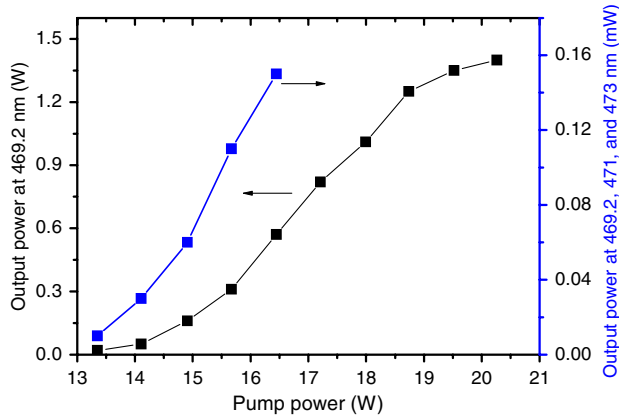


Fig. 4. (Color online) Output power curves for single-wavelength and multiwavelength laser operation versus incident pump power.

LBO crystal, one cannot obtain frequency doubling at 946 nm. However, by setting the LBO at an angle of $\Delta\phi = -0.6^\circ$, an effective frequency doubling at 946 nm can still be achieved.

To confirm the theoretical conclusions, we first achieved laser operation at 946 nm without glass etalon inside the V-shaped cavity. A maximum output power of up to 1.1 W at 473 nm was obtained by inserting and tilting the LBO. Compared with results of frequency doubling of 938.5 nm (as given in Section 4), the output power obtained by frequency doubling of 946 nm through the misadjustment of the LBO crystal is limited by extra reflection and extra walk-off losses. According to our calculations (see Fig. 2), this compensation can be also carried out by temperature tuning of the LBO crystal [20].

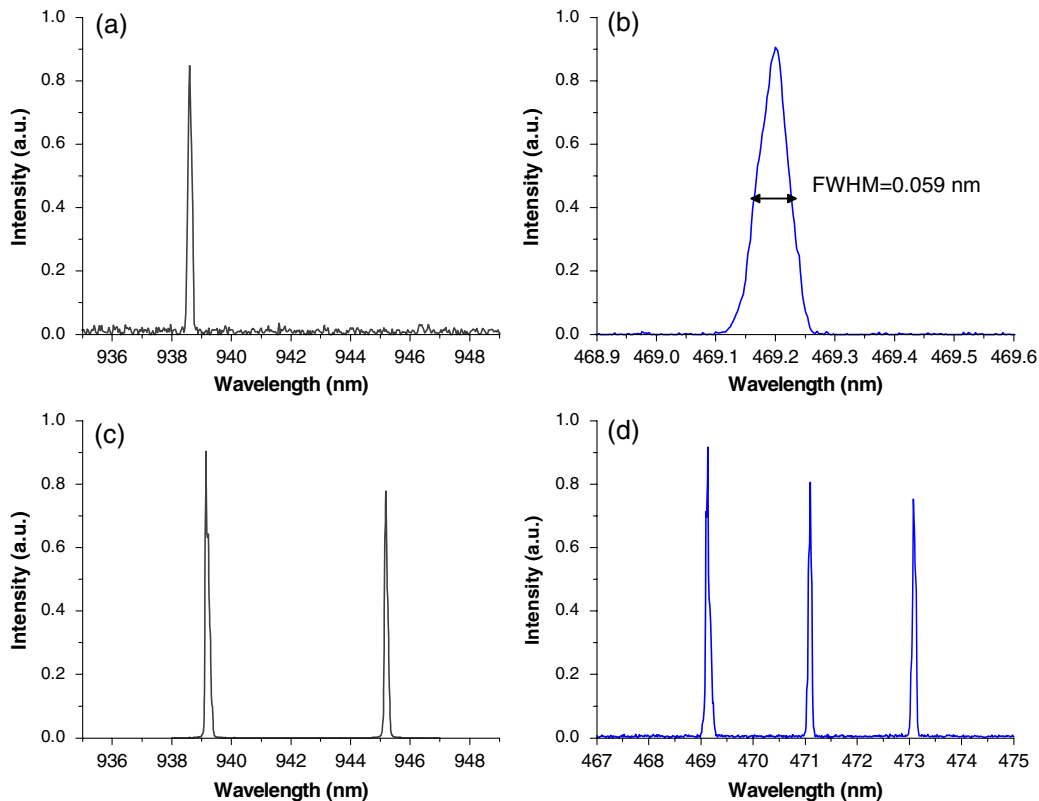


Fig. 5. (Color online) (a) 938.5 nm laser line selected with the glass etalon, (b) second-harmonic line generated at 469.2 nm, (c) simultaneous dual-wavelength lasing at 938.5 and 946 nm, and (d) simultaneous operation at 469, 471, and 473 nm.

As SHG is a special situation of sum-frequency generation (SFG) where the interactive wavelengths are equal, we also simulated the SFG within the LBO crystal with two wavelengths (938.5 and 946 nm) oscillating simultaneously in the cavity. In fact, thanks to the spectral proximity of the two wavelengths, the operating conditions of LBO for SFG of 938.5 and 946 nm [$\theta = 90^\circ$ and $\varphi = 19.6^\circ$ at 30°C with type I (ordinary-ordinary-extraordinary) phase matching] are very close to the SHG conditions at 938.5 nm. As shown in Fig. 2, the 471 nm radiation, which is the SFG of 938.5 and 946 nm, has only little coincidence with the SHG at 469.2 and 473 nm in the side lobes, which implies the possibility of a single 471 nm generation.

4. EXPERIMENTAL RESULTS AND ANALYSIS

Figure 3 gives the calculated transmission of the glass etalon at different wavelengths when a tilt angle of 8.8° was applied, which corresponds to a maximum transmission (100%) at 938.5 nm and sufficient extra losses to suppress the 946 nm laser emission. The tilt angle was adjusted by detecting the reflected rays out of the cavity, and it was found in good agreement with the calculated value. By setting the etalon to an angle of 8.8° and inserting the LBO crystal, the corresponding SHG at 469.2 nm was successfully generated, and the CW output power reached 1.4 W as recorded in Fig. 4. In the output direction, the IR and blue laser beams were measured to have a linear polarization of 11:1 and 25:1, respectively. It has to be noticed that, before inserting the LBO, the polarization ratio of the 938.5 nm wave was measured to be 2.1:1. Since YAG is an isotropic material and should emit unpolarized

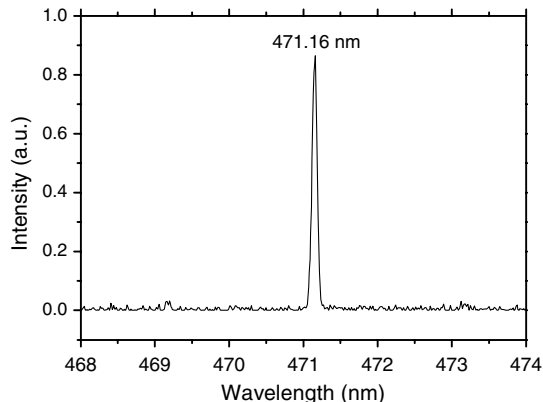


Fig. 6. 471.16 nm emission resulting from SFG of 946 and 938.5 nm, obtained by tilting the glass etalon.

radiation, the polarization of the 938.5 nm wave probably comes from the V-type asymmetric cavity. In fact, we did not observe any polarized output of the IR beam when using a linear (symmetric) cavity. However, it should be certainly interesting to scale the SHG output power with our LBO (type D) doubling crystal by inserting a Brewster plate and a quarter-wave plate between the input mirror and laser crystal, as reported in [5], which is not possible here because of the cavity compactness but will be our next investigation by using a longer Z-shaped cavity.

By tilting the glass etalon to an angle of around 8.0° and a synchronous angle tuning of the LBO crystal, we also achieved simultaneous triple-wavelength operation at ~469, ~471, and ~473 nm (see Fig. 5 for the registered spectra), as simulated above, where the simultaneous dual-wavelength lasing at 938.5 and 946 nm was first observed as a precondition for the simultaneous laser operation of the three blue laser wavelengths. The total maximum output power of three blue lasers can be modified by slightly tilting the glass etalon thus changing the different ratios of intracavity powers at 946 and 938.5 nm. We recorded a maximum output power of 150 mW with comparable intensities for each wavelength. Furthermore, by tilting the glass etalon and adjusting the LBO, the 469 and 473 nm laser actions could be nearly completely suppressed. The recorded spectrum of the 471.16 nm laser line is shown in Fig. 6. No output power curve at this wavelength has been recorded because laser operation was

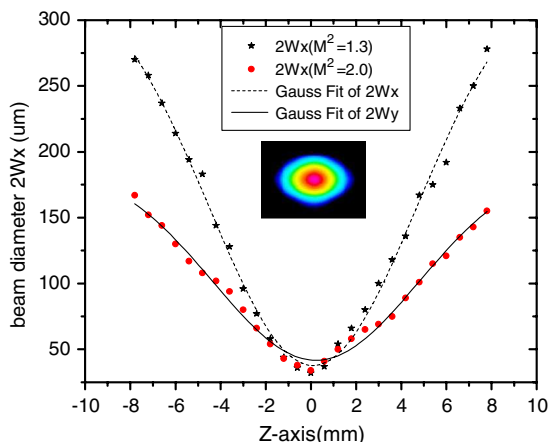


Fig. 7. (Color online) X and Y diameters of the output laser beam at 469.2 nm as a function of their Z-axis location.

only stable at specific pump power values. That is to say, the other two blue laser lines at 469 and 473 nm emerged when changing the pump power. We also found that, at different pump levels lower than around 16 W, the nearly single 471 nm laser operation could always be obtained by carefully adjusting the glass etalon and the LBO tilt angles.

A key factor that affects the stability of the blue output power is the temperature of the LBO crystal. Since the reduced size of the laser cavity hardly allowed the use of an oven to regulate the nonlinear crystal temperature, a Peltier cooler was thus used to control the temperature of the LBO. A stable blue output power was obtained by setting the temperature of the LBO crystal at 29.9 °C (±0.1 °C). Since the theoretical temperature bandwidth of LBO is 6.7K · cm, the 0.1 °C temperature fluctuation led to a good maximum output power stability of about 3.8% over half an hour for the 1.4 W blue laser at 469.2 nm.

The insertion losses *L* due to the glass etalon can be estimated by using the expression used in [21], i.e., $L = 2\theta R d / n w_o$, where θ is the incident angle, *R* is the etalon reflectivity for the angle θ , *d* the thickness, *n* the refractive index, and *w_o* the beam-waist radius onto the etalon. Therefore, in order to reduce the insertion losses as much as possible, a large laser beam waist onto the glass etalon is desirable. The glass etalon was inserted at a location where a mode radius of ~150 μm was found by ABCD calculations. This resulted in intracavity losses introduced by the glass etalon of the order of 0.71%.

We also noticed that, thanks to the etalon, the laser lines were substantially narrowed. The FWHM of the blue line at 469.2 nm was found to be smaller than 0.059 nm [Fig. 5(b)], which corresponds to the resolution limit of our optical spectrum analyzer (0.05 nm). Finally, the transverse spatial profile of the laser beam at 469.2 nm was measured with a Beamscope-P7. The beam propagation factors *M²* were found to be better than 1.3 and 2.0 in the X and Y directions, respectively (see Fig. 7).

5. CONCLUSION

In conclusion, we have demonstrated SHG and SFG in a diode-pumped V-type Nd:YAG-LBO laser cavity giving rise to 469.2, 471, and 473 nm laser emissions. A recorded output power of 1.4 W was obtained at 469.2 nm from the single-line operation of 938.5 nm. For the first time to the best of our knowledge, by allowing the two IR wavelengths at ~938.5 and ~946 nm to lase simultaneously, SFG and SHG were observed resulting in simultaneous multiwavelength operation at ~469, ~471, and ~473 nm. Power scaling at these blue wavelengths, especially at 938 nm, in order to pump Pr-doped materials could be obtained by inserting a polarization-selective element inside the cavity, and by better management of the thermal effects within the gain media, both ideas are still currently being investigated.

ACKNOWLEDGMENTS

This research was supported by the French National Research Agency (ANR) within the framework of the Matériaux Fluorés Structurés pour Sources Laser Rouge/Verte (FLUOLASE) research program and by a grant from the China Scholarship Council (CSC).

REFERENCES

1. B. M. Walsh, N. P. Barnes, R. L. Hutcheson, R. W. Equall, and B. Di Bartolo, "Spectroscopy and lasing characteristics of Nd-doped $\text{Y}_3\text{Ga}_x\text{Al}_{(5-x)}\text{O}_{12}$ materials: application toward a compositionally tuned $0.94\ \mu\text{m}$ laser," *J. Opt. Soc. Am. B* **15**, 2794–2801 (1998).
2. A. Braud, F. S. Ermeneux, Y. Sun, R. L. Cone, R. W. Equall, R. L. Hutcheson, C. Maunier, R. Moncorgé, N. P. Barnes, H. G. Gallagher, and T. P. Han, "Nd-doped mixed scandium garnets for improved laser performance and compositional tuning from 937 to 946 nm," in *Advanced Solid State Lasers*, C. Marshall, ed., Vol. **50** of OSA Trends in Optics and Photonics (Optical Society of America, 2001), paper ME12.
3. S. G. P. Strohmaier, H. J. Eichler, C. Czeranowsky, B. Ileri, K. Petermann, and G. Huber, "Diode pumped Nd:GSAG and Nd:YGG laser at 942 and 935 nm," *Opt. Commun.* **275**, 170–172 (2007).
4. B. Xu, P. Camy, J. L. Doualan, R. Soulard, Z. P. Cai, and R. Moncorgé, "Efficient diode-pumped Nd:GGG laser operation at 933.6 and 937.3 nm," *Appl. Phys. B*, **106**, 19–24 (2011).
5. C. Czeranowsky, E. Heumann, and G. Huber, "All solid state continuous wave frequency-doubled Nd:YAG-BiBO laser with 2.8 W output power at 473 nm," *Opt. Lett.* **28**, 432–434 (2003).
6. Z. Quan, Y. Yao, L. Bin, D. Qu, and Z. Ling, "13.2 W laser diode pumped Nd:YVO₄/LBO blue laser at 457 nm," *J. Opt. Soc. Am. B* **26**, 1238–1242 (2009).
7. J. Gao, X. Yu, F. Chen, X. Li, R. Yan, K. Zhang, J. Yu, and Y. Wang, "12.0 W continuous-wave diode end-pumped Nd:GdVO₄ laser with high brightness operating at 912 nm," *Opt. Express* **17**, 3574–3580 (2009).
8. A. Richter, E. Heumann, G. Huber, V. Ostroumov, and W. Seelert, "Power scaling of semiconductor laser pumped praseodymium-lasers," *Opt. Express* **15**, 5172–5178 (2007).
9. P. Camy, J. L. Doualan, R. Moncorgé, J. Bengoechea, and U. Weichmann, "Diode-pumped $\text{Pr}^{3+}:\text{KY}_3\text{F}_{10}$ red laser," *Opt. Lett.* **32**, 1462–1464 (2007).
10. K. Hashimoto and F. Kannari, "High-power GaN diode-pumped continuous wave Pr^{3+} -doped LiYF_4 laser," *Opt. Lett.* **32**, 2493–2495 (2007).
11. S. Khiari, M. Velazquez, R. Moncorgé, J. L. Doualan, P. Camy, A. Ferrier, and M. Diaf, "Red luminescence analysis of Pr^{3+} doped fluoride crystals," *J. Alloys Compd.* **451**, 128–131 (2008).
12. F. Cornacchia, A. Di Lieto, M. Tonelli, A. Richter, E. Heumann, and G. Huber, "Efficient visible laser emission of GaN laser diode pumped Pr-doped fluoride scheelite crystals," *Opt. Express* **16**, 15932–15941 (2008).
13. D. Pabœuf, O. Mhibik, F. Bretenaker, Ph. Goldner, D. Parisi, and M. Tonelli, "Diode-pumped $\text{Pr}:\text{BaY}_2\text{F}_8$ continuous-wave orange laser," *Opt. Lett.* **36**, 280–282 (2011).
14. B. Xu, P. Camy, J. L. Doualan, Z. Cai, and R. Moncorgé, "Visible laser operation of Pr^{3+} -doped fluoride crystals pumped by a 469 nm blue laser," *Opt. Express* **19**, 1191–1197 (2011).
15. R. Koch, W. A. Clarkson, and D. C. Hanna, "Diode pumped CW Nd:YAG laser operating at 938.5 nm," *Electron. Lett.* **32**, 553–554 (1996).
16. S. Bjurshagen, D. Evekull, and R. Koch, "Generation of blue light at 469 nm by efficient frequency doubling of diode pumped Nd:YAG laser," *Electron. Lett.* **38**, 324–325 (2002).
17. T. Y. Fan, "Heat generation in Nd:YAG and Yb:YAG," *IEEE J. Quantum Electron.* **29**, 1457–1459 (1993).
18. S. Singh, R. G. Smith, and L. G. Van Uitert, "Stimulated emission cross section and fluorescent quantum efficiency of Nd^{3+} in yttrium aluminium garnet at room temperature," *Phys. Rev. B* **10**, 2566–2572 (1974).
19. P. Li, D. Li, and Z. Zhang, "Efficient generation of blue light by intracavity frequency doubling of a cw Nd:YAG laser with LBO," *Opt. Laser Technol.* **39**, 1421–1425 (2007).
20. A. J. Lee, D. J. Spence, J. A. Piper, and H. M. Pask, "A wave-length-versatile, continuous-wave, self-Raman solid-state laser operating in the visible," *Opt. Express* **18**, 20013–20018 (2010).
21. M. Hercher, "Tunable single mode operation of gas lasers using intracavity tilted etalons," *Appl. Opt.* **8**, 1103–1106 (1969).